Fusing Cyclopentadiene and Ferrocene by Two Silyl Bridges Stereochemically Well-Defined Building Blocks for High-Nuclear Metallocenes

Monika Fritz, Johann Hiermeier, Norbert Hertkorn, Frank H. Köhler*, Gerhard Müller *) \#), Gabriele Reber *), and Oliver Steigelmann *)

Anorganisch-chemisches Institut der Technischen Universität München, Lichtenbergstraße 4, W-8046 Garching

Received January 15, 1991

Key Words: Ferrocenes / Cyclopentadienes, disilyl- / Silatropic rearrangement / Lithium cyclopentadienides / Metallocene, trinuclear, mixed-metal

The tetrahydro-4,4,8,8-tetramethyl-4,8-disila-*s*-indacenyl anion (LH) reacts with or without cyclopentadienyl anion (Cp^-) and $Fe_2Cl_4(THF)_3$ to give the mixed ferrocenes CpFe(LH) and $(LH)_2Fe$ in 50 and 63% yield, respectively. Near room temperature and in solution CpFe(LH) exists as a pair of enantiomers (*syn*-**3a/b**). According to an X-ray analysis both enantiomers are present in a single crystal. Compound **3** consists of a ferrocene linked to a cyclopentadiene by two Me_2Si groups such that the acidic Cp proton points towards the iron. Temperature-dependent NMR spectra show that *syn*-**3a** and *syn*-**3b** are non-rigid molecules which are interconverted by 1,2-silatropic bond shifts (E_a = 49.2 ± 2.9 kJmol^{-1}). Three more isomers (*anti*-**3a**, *anti*-**3b**, and the spiro derivative **3c**), though present only in low concentration, are engaged in the rearrangement. $(LH)_2Fe$ is also non-rigid and exists as a pair of diastereomers (**4a** and **4b**). The isomers of **3** and **4** undergo hydrolysis (e.g., *syn*-**3a/3b** gives [$(Me_2SiOSiMe_2)$Cp]FeCp (**5**) among others) and deprotonation. The latter yields CpFe(L^-) (**7**) and $(L^-)_2Fe$ (**8**), which are characterized by NMR spectroscopy. **7** forms crystals with $[Li(TMEDA)]^+$ as counterion, and an X-ray analysis shows that lithium and iron are located at opposite sides of the strongly folded ligand L. The reaction of **7** with $CrCl_2(THF)$ gives the trinuclear stacked metallocene **9** in 47% yield. **9** has two unpaired electrons which are located essentially in the center of the molecule.

A special class of high-nuclear organometallic compounds are organometallic polymers[1]. Their chemistry has been persued with considerable effort during the last two decades because they have promising properties like heat and electric conductivity[2], piezoelectric activity[3], activity in heterogeneous catalysis[4], rapid intramolecular charge transfer[5], and magnetic exchange[6]. In most cases, these properties have been achieved with ligand-assembled or polymer-bound organometallic fragments. Another concept is the synthesis of metal-containing ligands which may serve as building blocks in the complexation reaction with a variety of other metals. In order to realize the latter approach for transition-metal π-complexes we have focused our interest on the doubly bridged cyclopentadienes **1a** and **1b**[7], which we have been able to deprotonate selectively[8]. This offered the possibility of synthesizing metallocenes that are fused to cyclopentadienes. We have started testing this for iron derivatives and report on their synthesis, deprotonation, and further conversion to a paramagnetic Fe,Cr,Fe-trinuclear metallocene.

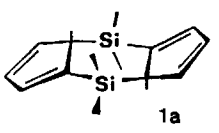

1a

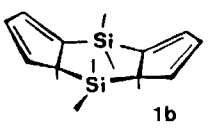

1b

*) Crystal structure analysis. — \#) New address: Fakultät für Chemie, Universität Konstanz, W-7750 Konstanz.

Starting Ferrocenes and their Deprotonation

Among the possibilities to generate the monoanion **2**[8] from the bridged cyclopentadienes **1a** and **1b** we have chosen the reaction with one equivalent of *n*BuLi. A colorless solution of **2Li** in THF is obtained and further treated as shown in Scheme 1. Thus, with solvated iron(II) chloride and an excess of CpNa, the ferrocene *syn*-**3a** (and its enantiomer *syn*-**3b**, cf. below) is obtained in 50% yield after removal of Cp_2Fe by sublimation and by separation from **4a** and **4b** by using medium-pressure liquid chromatography. The reaction with iron(II) chloride alone gives a 63% yield of the isomers **4a** and **4b** where two cyclopentadienes are fused to the ferrocene. An isomer ratio of 1:3 has been determined by NMR spectroscopy. However, the assignment of **4a** and **4b** to the structures in Scheme 1 is unclear.

The compounds *syn*-**3a/b**, **4a**, and **4b** are orange solids which are readily soluble in hexane, ethers, and other aprotic organic solvents; they are stable in dry air but rather moisture-sensitive because they contain allylic silyl groups. In an exploratory experiment we have added two drops of water to a solution of 10 mg of *syn*-**3a/b** in 1 ml of [D_6]acetone and followed the hydrolysis by NMR spectroscopy. After one week the signals of *syn*-**3a/b** have disappeared and a new compound has formed which is pure according to ^{13}C-NMR analysis. Its mass spectrum (*m/z* = 316, 100%, M^+; 301, 43% $M^+ - CH_3$) and NMR data [$\delta(^1H)$ = 0.15 and 0.37 (s and 6H each, CH_3), 4.22 (s, 5H, Cp), 4.30 (d, *J* = 2.2

Scheme 1. a: *n*BuLi, b: CpNa and $Fe_2Cl_4(THF)_3$; c: $Fe_2Cl_4(THF)_3$; for the enantiomer *syn*-**3b** of *syn*-**3a** cf. Scheme 3

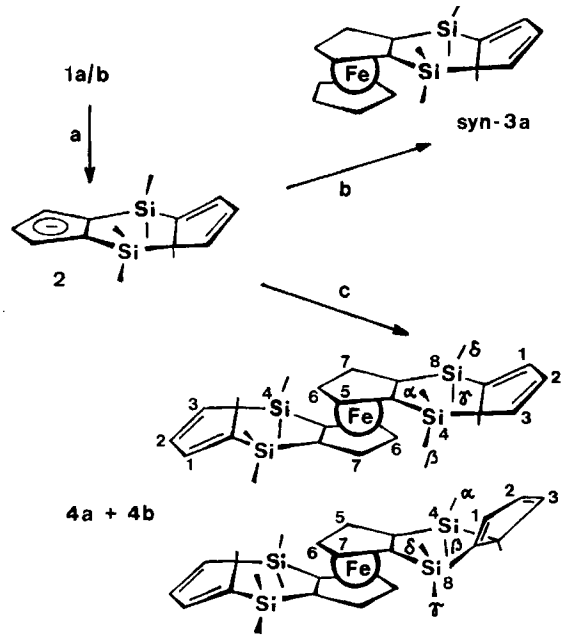

Hz, 2H, 3/5-H), 4.49 (t, J = 2.2 Hz, 1H, 4-H); $\delta(^{13}C)$ = 0.38 and 3.29 (CH_3) 69.18 (Cp), 73.42 (C-4), 77.86 (C-3/5), 75.93 (C-1/2)] are compatible with the silylated ferrocene **5**. In acetone **5** is slowly further converted to another ferrocene of the type [$(XMe_2Si)_2Cp$]FeCp. Its NMR data [$\delta(^1H)$ = 0.27 and 0.50 (s and 6H each, CH_3), 4.08 (s, 5H, Cp), 4.19 (d, J = 2.2 Hz, 2H, 3/5-H) 4.43 (t, J = 2.2 Hz, 1H, 4-H); $\delta(^{13}C)$ = 0.22 and 3.09 (CH_3), 68.78 (Cp), 71.43 (C-3/5), 76.92 (C-4), 82.40 (C-1/2)] are rather similar to those of **5** and its dimer[9] so that **6** (probably an oligomer of **5**) is a reasonable structural suggestion.

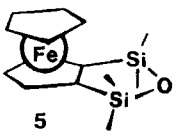
5

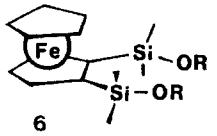
6

The cyclopentadiene units of *syn*-**3a**/**b**, **4a**, and **4b** can be deprotonated as shown in Scheme 2. No starting material has been detected by NMR after the reaction. The lithium derivative of the anion **7** is soluble in Et_2O and THF, but only amorphous yellow precipitates are obtained from these solution on cooling and/or concentration. Crystallization does, however, occur upon addition of TMEDA yielding the compound **7Li**(TMEDA).

When two equivalents of *n*BuLi are added to **4a** and **4b** dissolved in THF at −78°C, a clear solution is observed. slow warming up leads to a yellow precipitate which forms above −40°C, and which can be shown by NMR to contain the dianion **8**. When only one equivalent of *n*BuLi is used under otherwise equal conditions no precipitate appears. From this we conclude that the deprotonation of **4a** and **4b** is a stepwise process. From **8**, in contrast to **7**, crystals free of TMEDA can be obtained.

Scheme 2. a: *n*BuLi; the counterion of **7** and **8** is Li^+

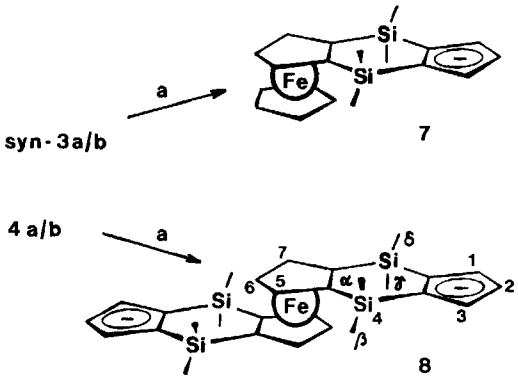

Dynamic Behavior and Further Spectroscopic Characteristics

In the mass spectra of mixtures of the ferrocenes *syn*-**3a**/**b** or **4a**/**b** the base peaks are due to the molecular ions, and only few fragment ions with medium intensity are visible. The experimental and calculated pattern of the molecular ions are in good agreement.

syn-**3a**/**b**, **4a**, and **4b** show temperature-dependent NMR spectra, as expected for cyclopentadienes being substituted by silyl and similar groups[10]. As a representative example *syn*-**3a** and *syn*-**3b** are studied in detail. At 10°C and below in [D_8]toluene each of the fifteen non-equivalent carbon atoms gives rise to a separate signal (Figure 1). On heating

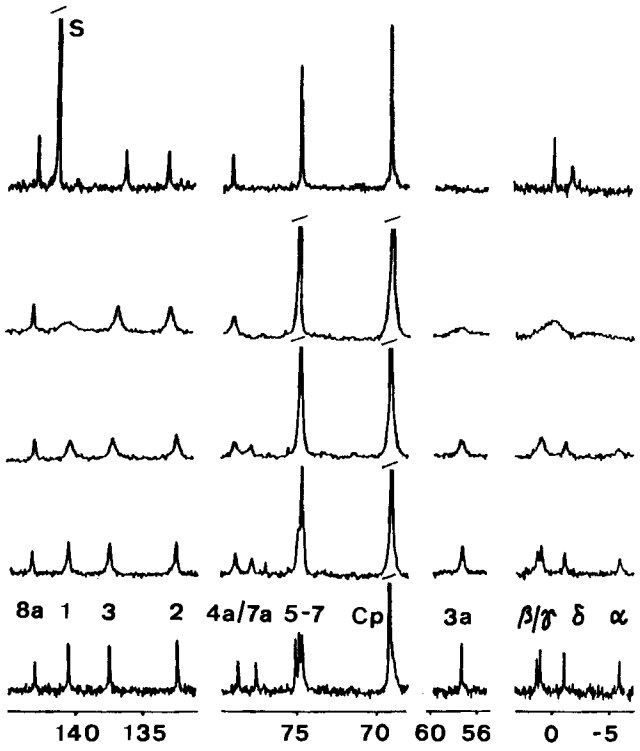

Figure 1. ^{13}C-NMR spectra of *syn*-**3a**/**b**. From bottom to top: 10, 35, 50, 75 and 160°C. Solvent: C_6D_6 except for 160°C with [D_{10}]biphenyl. δ scale. Assignment of C-5-7 see Table 1. S = Solvent

all signals broaden but signal collapse only occurs for the pairs C-4a/7a and C-5/7 of the ferrocene part as well as C-α/δ and C-β/γ. This contrasts with **2** where averaged signals are also observed for the cyclopentadiene part[8]. At 180°C (in [D_{10}]biphenyl) the remaining signals have resharpened except those for C-1 and C-3a that are still too broad to be detected.

The NMR results show some remarkable similarities and differences between *syn*-**3a**/**3b** and **2**. We can therefore shorten the discussion by referring to the arguments given for **2**[8]. Thus, only 1,2-silatropic shifts between C-3a and C-8a or C-1 and C-8a are responsible for the dynamic behavior which is summarized in Scheme 3.

Scheme 3. Silatropic bond shifts in **3a**/**b**. The numbering represents the identity of the nuclei after bond shifts; it follows the usual convention only for *syn*-**3a** which has been arbitrarily chosen as starting isomer

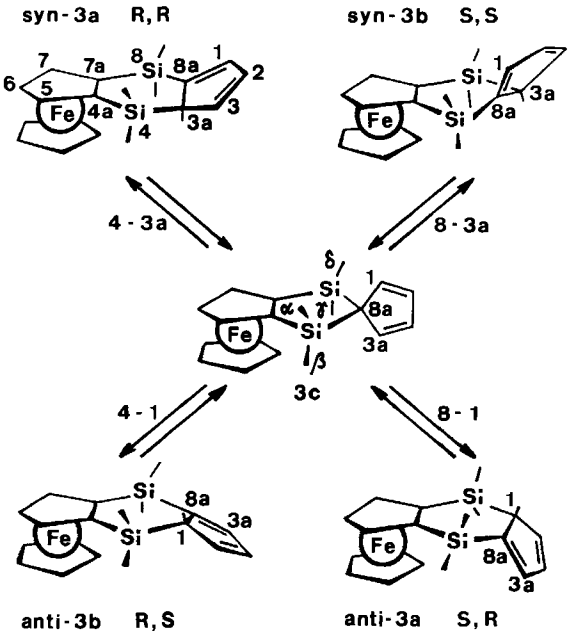

Any of the interconversions of the four low-symmetry isomers must proceed via the spiro derivative **3c**. The numbers of the two atoms, which make up the new bonds, are given with the arrows. Starting from **3c**, isomers are conceivable where 3a-H is *syn* or *anti* with respect to CpFe and where the centers of central and planar chirality (C-3a and the ferrocene unit) yield two pairs of enantiomers *syn*-**3a**/**b** and *anti*-**3a**/**b** and two pairs of diastereomers, *syn*-/*anti*-**3a** and *syn*-/*anti*-**3b** (the *R,S* nomenclature of ref.[11] has been adopted in Scheme 3). Since only one set of signals is present in the low-temperature limiting ^{1}H and ^{13}C spectra, only enantiomers are seen, and the concentration of either the *syn*- or the *anti*-isomers must be immeasurably small. The δ(^{1}H) values discussed below point to the predominance of the *syn*-isomers.

It is now easy to see why the coalescence of the ^{13}C signals of *syn*-**3a**/**b** is different from that of **2**. The rearrangement *syn*-**3a** ⇄ *syn*-**3b** exchanges C-4a and C-7a as well as C-5 and C-7 whereas C-1/2/3/3a/8a retain their identity. For **2** an additional coalescence of the signals of C-1/3a and C-2/3 is observed. This does not occur for *syn*-**3a**/**b** because it requires a *syn,anti*-rearrangement with a *high* concentration of the *anti*-isomer which is not observed. The fact that the signals of C-1/2/3/3a/8a broaden without signal collapse on increasing the temperature is due to the exchange of the *syn*-isomer with other isomers at very *low* concentration ("hidden partner exchange"[12]). Three hidden partners (**3c**, *anti*-**3a**, and *anti*-**3b**) are present besides *syn*-**3a**/**b** whereas only one (the spiro derivative analogous to **3c**) is found for **2**. That *anti*-**3a**/**b** are more important as hidden partners than **3c** is derived from the differential broadening of the signals of C-1/2/3/3a/8a as follows. The maximum half width Δ^{max} of a broadened signal is given by $\Delta^{max} = p \cdot \Delta\delta$ (p is the population of the hidden isomer, $\Delta\delta$ is the signal shift difference of the engaged nuclei of the hidden and the highly populated isomer)[12a]. Excessive broadening is expected only if allylic and olefinic C-atoms are interchanged resulting in $\Delta\delta \approx 75-87$ [taken from Table 1 and 5,5-bis(trimethylsilyl)cyclopentadiene[13]], whereas for the interchange of the olefinic C-atoms $\Delta\delta \approx 1-12$. Scheme 3 shows that C-3a/8a or C-1/3a should be most affected depending on whether **3c** or *anti*-**3a**/**b** dominate as hidden partners. The experiment clearly sorts out *anti*-**3a**/**b** (Figure 1).

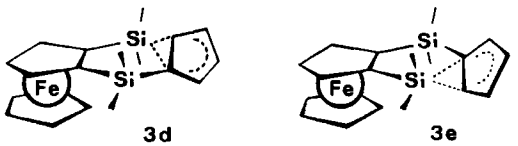

The fact that *syn*-**3a**/**b** are lower in energy than *anti*-**3a**/**b** (cf. below) implies that two transition states exist for the rearrangements; the lower one should be that with a *syn*-type proton as in **3e** rather than with an *anti*-type proton as in **3d**. The barrier has been determined from the field and temperature dependence of the signal coalescence of C-4a/7a and C-5/7 (Experimental) to be $E_a = 49.2 \pm 2.9$ kJmol^{-1}. Within the error limits this equals the barrier of **2**, which means that the influence of the CpFe moiety is small.

Important additional conclusions are based on the ^{1}H-NMR spectra. In order to meet the need for well separated signals and variable temperature data various solvents have to be used (cf. Table 4, Experimental). On replacing $CDCl_3$ or [D_8]dioxane by aromatic solvents notable changes of the signal shifts are seen only for the ferrocene part as might be expected from the interaction between aromatic molecules. In particular, the signal of the stereochemically interesting proton 3a-H has an almost constant shift near 4.2 ppm for $T \leq 20$°C. This is about 0.7 ppm to higher frequency as compared to the corresponding signals of **1a** and **1b** and must be ascribed to the anisotropy of the diamagnetic susceptibility of the ferrocene. The "NMR mapping" of ferrocenes[14] shows that a deshielding of 3a-H is only expected if it is located *syn* to the ferrocene. It must be noted, however, that a related series of bis(benzene)chromium com-

pounds establishes deshielding zones in- and outside the sandwich[15].

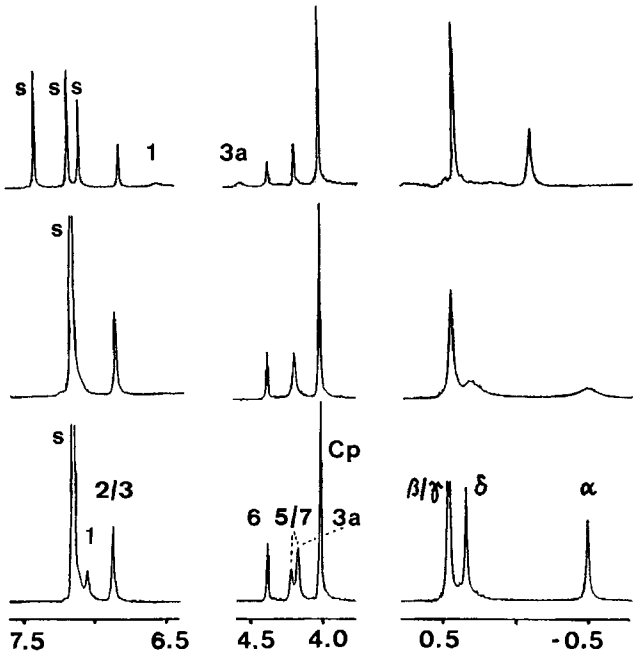

Figure 2. ^{1}H-NMR spectra of *syn*-**3a/b**. Bottom: At 25 °C in C_6D_6. Middle: At 60 °C in C_6D_6. Top: At 140 °C in [D_{10}]biphenyl. δ scale, S = solvent

The ^{1}H-NMR spectrum of *syn*-**3a/b** at various temperatures (Figure 2) shows an accidental coincidence of the signals of 5-H or 7-H and 3a-H as well as of 2-H and 3-H in C_6D_6 at 25 °C. The latter two signals split around 50 °C before coalescence occurs above 60 °C. In accordance with the symmetry requirements a pairwise coalescence is observed for the MeSi signals. This establishes the assignment of δ-H because its coalescence partner is α-H. The latter is identified by a comparison with **1a** and **1b**[8] which also help to assign other resonances. The existence of the *syn,anti*- besides the *syn,syn*-rearrangement discussed above for **3a/b** is particularly well documented by the signals of 1-H and 3a-H. Their shift difference for the *syn*- and *anti*-isomer is so big that, in the temperature range 60 °C ≤ T < 140 °C, the line widths are increased beyond detection of the resonances (Figure 2, middle). On the other hand (and in contrast to C-1 and C-3a), the shift difference is small enough as to allow the signals of 1-H and 3a-H reappear at 140 °C (Figure 2, top). In addition, they have moved towards the resonance position of their (hidden) exchange partners which are more populated at 140 °C. This trend continues on heating to 180 °C.

The ^{13}C-NMR data of all new compounds are collected in Table 1. Starting with **3a/b**, the less trivial signal assignment for C-1/2/3/α follows that of **1a** and **1b**[8], C-δ is recognized as the coalescence partner of C-α, and C-6 is distinguished from C-5/7 because the latter show coalescence at elevated temperature. The signal assignment for **4a** and **4b** is based on that of **3a/b**. From the results on *syn*-**3a/b** we conclude that in **4a** and **4b** only the *syn*-conformation

Table 1. ^{13}C-NMR data[a] of compounds **3**, **4**, **7**, and **8**

position[b]	syn-**3a/b**[c]	**4a**[d]	**4b**[d]	**7**[e]	**8**[f]
1	140.65 (161.7)	140.57	140.95	115.19	114.95
2	132.39 (162.9)	132.30	132.36	108.80	108.55
3	137.52 (166.3)	138.36	138.24	115.19	114.95
3a	57.68 (131.7)	57.51	58.06	118.01	118.18
8a	143.23	143.51	143.23	118.01	118.18
Cp	69.07 (175.0)			68.92	
5	74.54[g] (173.3)	75.76[h]	75.97[h]	74.85	76.09
7	74.96[g] (172.8)	77.11[h]	76.39[h]	74.85	76.09
6	74.72 (173.3)	76.32[h]	77.26[h]	72.18	74.74
4a[i]	77.48	77.63	77.26	80.48	79.04
7a[i]	78.58	78.73	79.27	80.48	79.04
α	-5.86 (120.2)	-5.98	-5.94	5.61	5.51
δ	-1.09 (119.9)	-0.74	-0.52	5.61	5.51
β[i]	0.95 (119.3)	0.71	-0.75	-0.94	0.03
γ[i]	1.28 (119.6)	1.38	1.00	-0.94	0.03

[a] Shifts in δ values, in parentheses $^1J(^{13}C,^1H)$ in Hz. — [b] Cf. Schemes 1 and 2. — [c] In C_6D_6 at 5 °C. — [d] In [D_8]THF at −61 °C; cf. text for the identity of **4a/b**. — [e] In [D_8]THF/TMEDA at 30 °C. — [f] In [D_8]THF at 30 °C. Interchange not excluded between [g] C-5/7, [h] C-5/6/7, and [i] C-4a/7a and C-β/γ of **3a**, **4a** and **4b**.

(3a-H close to Fe) is realized. Then the two signal sets in the ^{13}C-NMR spectrum must be due to the diastereomers shown in Scheme 1. In Table 1 the less abundant isomer is **4a**. However, it is unclear which of the two structures in Scheme 1 belongs to **4a** and **4b**, respectively. Deprotonation of **3a/b** and **4a/b** removes the dynamic behavior and leads to fewer signals in the NMR spectra of **7** and **8** that are in accord with the expected C_s and C_{2h} symmetry; the signals of C-α/δ and C-β/γ can be distinguished after comparison with the dianion of **1a/b**[8]. All ^{1}H-NMR data are given in the Experimental.

For mixtures of **3a** and **3b** and of **4a** and **4b** the cyclovoltammograms have been recorded in THF (10^{-4} mol^{-1}) relative to the saturated calomel electrode (electrolyte nBu$_4$NPF$_6$, 25 °C, scan rate 50 mVs^{-1}). The half-wave potentials are $\Delta E_{1/2}$ = 602 and 670 mV which means that, as

compared to Cp_2Fe ($\Delta E_{1/2}$ = 570 under the same conditions), an increasing number of silyl groups renders the ferrocene less oxidizable. This parallels the effect of other electron-withdrawing substituents[16]. The difference between the oxidation and the reduction potential is the same for all experiments. Hence **4a** and **4b** must have very similar $\Delta E_{1/2}$ values.

Crystal Structures

The question whether the enantiomers **3a/b** have *syn*- or *anti*-conformation is definitely settled by X-ray analysis which establishes (Figure 3) the *syn*-conformation (Table 2). Complex *syn*-**3** crystallizes as a racemate, i.e., both enantiomers *syn*-**3a** and *syn*-**3b** are present in a single crystal. Figure 3 shows only one enantiomer, the *S,S*-configurated *syn*-**3b**.

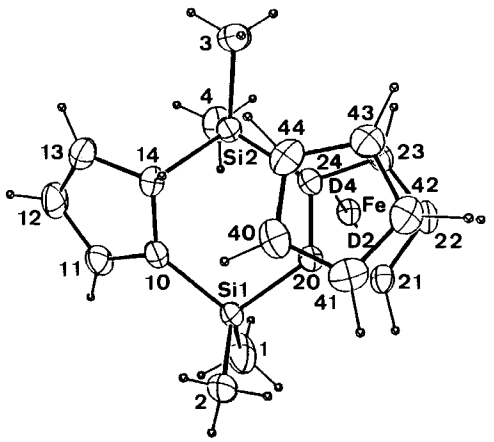

Figure 3. Molecular structure of one of the enantiomers of *syn*-**3** (*syn*-**3b**; for discussion see text) in the crystal and atomic numbering scheme adopted (ORTEP, displacement ellipsoids at the 50% probability level, H atoms with arbitrary radii)

Table 2. Selected distances [Å] and angles [°] for *syn*-**3a/b**

C10-C11	1.366(1)	Si1-C20	1.864(1)
C11-C12	1.439(1)	Si2-C3	1.875(1)
C12-C13	1.353(1)	Si2-C4	1.859(1)
C13-C14	1.481(1)	Si2-C14	1.909(1)
C14-C10	1.509(1)	Si2-C24	1.867(1)
Si1-C1	1.862(1)	Fe-D2[a]	1.65
Si1-C2	1.869(1)	Fe-D4[a]	1.66
Si1-C10	1.856(1)		
C10-C14-Si2	107.1(1)	C10-C11-C12	110.7(1)
C14-Si2-C24	105.1(1)	C11-C12-C13	109.1(1)
Si2-C24-C20	124.0(1)	C12-C13-C14	108.9(1)
C24-C20-Si1	124.4(1)	C13-C14-C10	104.6(1)
C20-Si1-C10	105.0(1)	C14-C10-C11	125.6(1)
Si1-C10-C14	125.6(1)	D2-Fe-D4	178.2

[a] Centroids of the Cp rings.

The cyclopentadiene fragment of *syn*-**3a/b** is very similar to those of **1a**[17], only the angle of fold (C10,C11,C12,C13)/(C10,C14,C13) = 2.5° is somewhat smaller. In the ferrocene moiety the distances and angles are in the usual range. Thus in the unsubstituted Cp ring, the C–C lengths are in the range 1.412(1)–1.428(1) Å (mean value 1.42 Å), and the Fe–C distance is 2.045(1)–2.060(1) Å (mean value 2.05 Å); in the substituted Cp ring the C–C distances lie between 1.418(1) and 1.453(1) Å (mean value 1.43 Å), and Fe–C is 2.038(1)–2.062(1) Å (mean value 2.05 Å), which transforms into distances of 1.65 and 1.66 Å between Fe and the Cp centroids D2 and D4. The ferrocene moiety is slightly bent (D2–Fe–D4 178°), the interplanar angle of the Cp rings is 2.5°, and their relative orientation is close to eclipsed with a mean deviation (9.1°) like that in Cp_2Fe at low temperature[18].

The most remarkable feature is the orientation of the methyl groups. The *syn*-methyl groups (C2 and C3) are bent away from the ferrocene, so that their interaction with Cp is minimized, and yet they are still rather close to it (C2···C40 3.665, C3···C44 3.793 Å). As a consequence the distance between the *syn*-methyl groups is much longer (C2···C3 6.564 Å) than that between the *anti*-methyl groups (C1···C4 4.639 Å), and the substituents at Si2 and C14, including the stereochemically important H14, are staggered. A model shows that in *anti*-**3b** corresponding distortions lead to an eclipsed arrangement of the substituents at Si2 and C14, thereby destabilizing this isomer. In

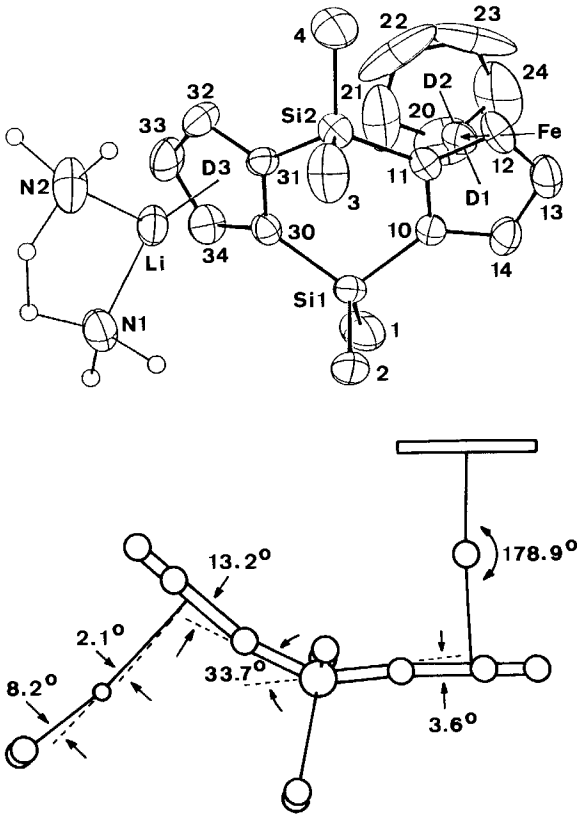

Figure 4. Molecular structure of **7Li**(TMEDA) (H atoms omitted; disordered TMEDA-C atoms with arbitrary radii, all other atoms with displacement ellipsoids). The numbering refers only to the X-ray results and to C atoms if not stated otherwise. Bottom: Selected interplane angles and bending of the Li(TMEDA) and the ferrocene fragment

context with the characteristic NMR signal shift of H14 (3a-H in Scheme 1) it is worth noting that the distance D2···H14 is 3.962 Å and that the angle Fe–D2–H14 is 65.5°. Hence, H14 lies between the Cps roughly at the same height as iron which means well in the deshielding range (cf. previous chapter).

Table 3. Selected distances [Å] and angles [°] for **7Li**(TMEDA)

Si1-C30	1.839(5)	Si1-C2	1.868(8)
C30-C31	1.457(8)	Si2-C3	1.883(7)
C31-Si2	1.840(6)	Si2-C4	1.857(6)
Si2-C11	1.857(5)	Li-N1	2.14(1)
C11-C10	1.457(8)	Li-N2	2.18(1)
C10-Si1	1.868(6)	Li-D3[a]	1.948
Si1-C1	1.866(8)	Fe-D1[a]	1.644
		Fe-D2[a]	1.651
Si1-C30-C31	123.1(4)	C11-C10-Si1	123.9(4)
C30-C31-Si2	124.5(4)	C10-Si1-C30	106.0(2)
C31-Si2-C11	105.3(3)	D1-Fe-D2	178.9
Si2-C11-C10	122.8(4)		

[a] Centroids of the Cp rings.

Considerable structural changes occur when *syn*-**3a/b** is deprotonated. Figure 4 shows the carbanion **7** with lithium stabilized by TMEDA as counterion. Alternatively **7Li**(TMEDA) may be looked at as a mixed main group/transition metal derivative of two bridged Cps. The CpLi(TMEDA) fragment has distances [C–C 1.40(1)–1.457(8) Å, mean value 1.42 Å; Li–C 2.25(1)–2.34(1) Å, mean value 2.29 Å] similar to those of the Li(TMEDA) derivative of doubly deprotonated **1a/b**[8] and of other silylated Cp anions[19]. The unsubstituted Cp ring [C–C 1.32(2)–1.40(2) Å, mean value 1.36 Å, Fe–C 2.006(9)–2.028(8) Å, mean value 2.02 Å] shows considerable disorder as is evident from the large displacement ellipsoids, particularly those of C atoms C22/C23. Because the disorder cannot be resolved with split-atom models conventional refinement with anisotropic displacement parameters has been carried out which results in some artificially shortened bond lengths. The non-uniformity of the displacement ellipsoids of atoms C20–C24 (Figure 4) points to the absence of pure rotational disorder of the Cp ring. The situation is reminiscent of that in the disordered high-temperature modifications of ferrocene where only the superposition of multiple ring positions could account for the observed disorder[20]. The substituted Cp is not unusual [C–C 1.41(1)–1-457(8) Å, mean value 1.43 Å; Fe–C 2.038(7)–2.052(5) Å, mean value 2.045 Å], both Cps include an interplanar angle of only 0.8°, the bending (D1–Fe–D2 178.9°) is also small, and their mean deviation from the eclipsed conformation is 16.9°. Further details are given in Table 3.

As illustrated in a side view of **7Li**(TMEDA) (Figure 4, bottom) the bridging ligand suffers from a striking distortion. Thus, the interplanar angles sum up to a deviation of 43.3° from the parallel arrangement of the two Cp rings. The distortion is mainly induced by the steric congestion between the CH_3Si groups (C1/4) and CpFe. It leads to a distance between C1 and C4 which is longer than that between C2 and C3 (cf. discussion for *syn*-**3b**) and, thereupon, to a folding at Si1–Si2 such that the six-membered central ring adopts a boat conformation. The interaction between the Li(TMEDA) fragment and the CH_3Si groups (C2/3) is minimized by the folding at Si1–Si2 (146.3°) and at C30–C31 (166.8°), by the angle between Li–D3 and the normal to the Cp ring (2.1°) as well as by the angle between the plane Li,N1,N2 and the line Li–D3 (171.8°). In view of these features it is clear that the two metals prefer to be located in an *anti*-position.

TMEDA takes an asymmetric position relative to the closest Cp. Thus, the lines N1–N2 and C30–C31 are not parallel (deviation 12.7°) and the distance of N1 and N2 from the Cp ring is 3.60 and 3.44 Å, respectively. The methylene carbon atoms of the coligand TMEDA show the usual disorder leading to rather ill-defined methyl group positions.

The Paramagnetic Trinuclear Metallocene CpFeLCrLFeCp (9)

The building block concept mentioned in the introduction has been realized with the anion **7**, and by its reaction with solvated chromium(II) chloride (Scheme 4). The procedure can be simplified by starting from a mixture of *syn*-**3a/b** and the inevitable Cp_2Fe. Later, the latter can be easily removed from **7** by extracting it with hexane. The trinuclear stacked metallocene **9** is isolated in 47% yield as a very air-sensitive orange-red microcrystalline product. Its molecular formula and purity are confirmed by elemental analysis and by the mass spectrum which shows a good agreement between the experimental and calculated isotope pattern of the molecular ion.

Scheme 4. a: *n*BuLi; b: $CrCl_2$(THF)

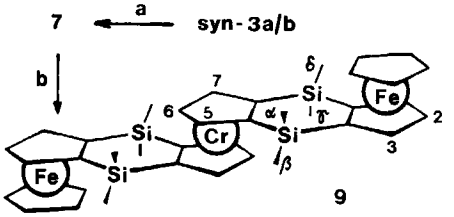

The structure and the magnetism of **9** follow from the ^{1}H-NMR spectrum (Figure 5). The two signals at very high frequency appear in a range that is typical of chromocenes including a silylated derivative[21]. Therefore, they must be assigned to 5/7-H and 6-H, and the molecule must have two unpaired electrons localized mainly on the central metallocene ($^3E_{2g}$ ground state). There are five more signals that have temperature-dependent signal shifts and that can be assigned on the basis of their relative areas as shown in Figure 5. An independent argument for the assignment is the spin delocalization. Only little spin density is expected on the ferrocene due to the number and the unfavorable orientation of the intervening bonds. In fact, the shift of the

signals of 1/3-H, 2-H, and Cp is small. The methyl groups are oriented such that they experience hyperconjugative spin transfer[22] from the central chromocene and possibly some dipolar interaction. Hence, their signals are more strongly shifted.

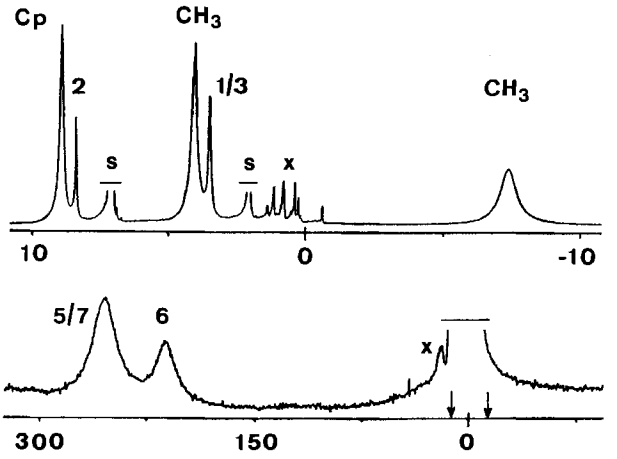

Figure 5. ^{1}H-NMR spectra of **9** dissolved in [D_8]toluene. Bottom: Full spectrum, 31°C, 200 MHz, high-power mode; the range indicated by the arrows has been expanded in the top: 22°C, 270 MHz, high-resolution mode. δ scales, S = solvent, X = probehead signal and impurities (top)

This work has been supported by *Deutsche Forschungsgemeinschaft*, by *Fonds der Chemischen Industrie*, and by *Wacker Chemie GmbH*. We are indebted to *J. Riede* for collecting the X-ray data.

Experimental

Air- and water-sensitive compounds were handled under purified nitrogen or argon using Schlenk tube techniques. As for lithium and chromium compounds the glassware was flame-dried in vacuo. All solvents were dried by standard methods and saturated with inert gas. Kronwald medium-pressure liquid chromatography equipment including Sepapress HPP-100/50 pump, HPD pulsation dampener, Sepacon PCU 60 pressure control unit, Sepachrom FPGC glass column (diameter 26 mm, length 50 cm) was used for preparative separation; stationary phase Merck silica gel 60 (15–40 μm), solvent pentane, pressure 3–15 bar. – MS: Varian MAT 311A (EI, 70 eV). – Cyclovoltammograms: electrochemical station consisting of a home-made cell with Pt wire working electrode, Pt net counter electrode and saturated calomel electrode, a standard potentiostat Wenking ST 72, a voltage scan generator Wenking VSG 72, and a Hewlett-Packard HP 7004B plotter. – NMR: Jeol JNM GX 270 and Bruker CXP 200, for variable-temperature NMR spectra, the temperature was measured as described previously[23]. All signal shifts were measured relative to solvent signals and calculated relative to TMS using δ(^{1}H) 7.24, 3.53, 7.15, 2.10, 1.73, and 7.40 for $CHCl_3$, dioxane, benzene, $C_6D_5CD_2H$, 3/4-H of THF, and 2/6-H of biphenyl, δ(^{29}Si) 6.87 for $[(CH_3)_3Si]_2O$, and δ(^{13}C) 128.0 and 25.8 for C_6D_6 and C-2/5 of [D_8]THF.

(Cyclopentadienyl)(syn-1,2,3,3a,8a-η^5-3a,4,7a,8-tetrahydro-4,4,8,8-tetramethyl-4,8-disila-s-indacen-7a-yl)iron (*syn*-**3a/b**): To the mixed solutions of 6.0 mmol of **2**[8] in 30 ml of THF and 30 mmol of CpNa in 70 ml of THF was added 4.3 g (9.2 mmol) of $Fe_2Cl_4(THF)_3$ with stirring at 25°C. The reaction mixture was stirred for 1 h after which time an orange suspension was obtained. THF was stripped in vacuo, the remainder extracted with one 100-ml and four 10-ml portions of pentane, and from the combined extracts the solvent was removed. When subjected to sublimation (40°C/2 Pa) most of the inevitable Cp_2Fe could be separated. The residue was dissolved in a few ml of pentane and chromatographed by MPLC. The first band contained a small quantity of Cp_2Fe, the second band was collected and freed from pentane to give an orange powder of *syn*-**3a/b**. Yield 1.1 g (50% relative to **2**). Alternatively, *syn*-**3a/b** could be obtained by fractional sublimation as orange crystals, m.p. 93°C. – MS, *m/z* (%): 364 (100) [M^+], 349 (73) [$M^+ - CH_3$], 298 (7) [$M^+ - C_5H_6$], 283 (17) [$M^+ - C_5H_6 - CH_3$], 282 (11) [$M^+ - C_5H_6 - CH_3 - H$], 268 (3) [$M^+ - C_5H_6 - 2\,CH_3$], 121 (4) [$CpFe^+$]; isotope pattern of M^+, *m/z* (% calcd./found): 362 (6.3/6.7), 363 (2.0/2.8), 364 (100/100), 365 (34.2/34.0), 366 (12.5/12.3), 367 (2.6/2.7). – ^{1}H NMR: see Table 4. – ^{29}Si NMR (THF, 30°C): δ = −0.48 (Si-4), −13.99 (Si-8).

$C_{19}H_{24}FeSi_2$ (364.4)
Calcd. C 62.62 H 6.64 Fe 15.41 Si 15.33
Found C 62.04 H 6.71 Fe 15.40 Si 15.0

Table 4. ^{1}H-NMR signal shifts of *syn*-**3a/b**

position[a]	solvent and temperature				
	$CDCl_3$ −60 °C	[D_8]-dioxane 27 °C	C_6D_6 20 °C	[D_8]-toluene 0 °C	[D_{10}]-biphenyl 180 °C
1-H	7.01	6.98	7.06	6.99	6.42
2-H	6.83[c]	6.78	6.88[f]	6.88	6.77
3-H	6.90[c]	6.88	6.88[f]	6.88	6.77
3a-H	4.18	4.18	4.18	4.14	4.63
5/7-H[b]	4.40[d,e]	4.39	4.23	4.21	4.21
	4.33[d,e]	4.33	4.18	4.17	4.21
6-H	4.61[d]	4.57	4.39	4.38	4.39
Cp	4.21	4.23	4.03	4.02	4.03
α-H	-0.71	-0.71	-0.49	-0.50	-0.09
β/γ-H[b]	0.54	0.57	0.47	0.47	0.43
	0.43	0.47	0.45	0.45	0.43
δ-H	0.23	0.22	0.35	0.35	-0.09

[a] For numbering cf. Scheme 1. – [b] Assignment not assured. – [c] $^3J_{2,3}$ = 4.5 Hz. – [d] $^3J_{5/7,6}$ = 2.1 Hz. – [e] $^4J_{5,7}$ = 0.9 Hz. – [f] Separate signals (Δδ = 0.005) at 50 and 60°C.

Bis(1,2,3,3a,8a-η^5-3a,4,7a,8-tetrahydro-4,4,8,8-tetramethyl-4,8-disila-s-indacen-3a-yl)iron (Isomers **4a** and **4b**): 1.29 g (2.3 mmol) of $Fe_2Cl_4(THF)_3$ was poured at 25°C into a stirred solution of 10.0 mmol of **2**[8] in 100 ml of THF. After stirring the brown reaction mixture for 1 h THF was removed under reduced pressure and the solid extracted several times with toluene. The combined extracts were concentrated to 20 ml, and 20 ml of pentane was added. Cooling to −25°C gave a light orange precipitate which was washed with 10 ml each of pentane and ether. After drying in vacuo an orange powder consisting of two isomers (NMR) was obtained. Yield 1.71 g (63% relative to **2**); m.p. 190–192°C (rapid heating), dec. above 140°C (slow heating). – MS, *m/z* (%): 542 (100) [M^+], 298 (18) [M^+ – ligand], 283 (6) [M^+ – ligand – CH_3]; isotope pattern of H^+, *m/z* (% calcd./found): 540 (6.2/6.2), 541 (3.3/3.4), 542 (100/100), 543 (5.4/52.6), 544 (27.7/26.7), 545 (9.1/8.6), 546 (2.6/2.4).

$C_{28}H_{38}FeSi_4$ (542.8)
Calcd. C 62.96 H 7.06 Fe 10.29 Si 20.70
Found C 61.89 H 6.97 Fe 9.94 Si 20.7

*Reaction of syn-***3a/b** *with Methyllithium:* 0.80 g (2.2 mmol) of ***syn*-3a/b** was dissolved in 50 ml of Et_2O and the solution cooled to 0°C. To this solution was added dropwise 1 ml of a 2.20 M solution of MeLi in Et_2O. After stirring at 0°C for 1 h a light orange solid had formed which completely dissolved on warming to 25°C. Cooling to −78°C overnight gave a precipitate from which the solvent was decanted. The remaining solid was washed three times with 25-ml portions of cold pentane and dried in vacuo. Yield 0.75 g (92%) of an orange material which, after dissolution in [D_8]THF, exhibited the NMR signals of *(cyclopentadienyl)(1,2,3,3a-η⁵-3a,4,7a,8-tetrahydro-4,4,8,8-tetramethyl-4,8-disila-s-indacene-3a,7a-diyl)iron* anion (**7**). – ^{1}H NMR ([D_8]THF, 25°C): δ = 6.21 (d, $J_{1/3,2}$ = 2.8 Hz, 2H, 1/3-H), 5.99 (t, $J_{2,1/3}$ = 2.8 Hz, 1H, 2-H), 4.22 (d, $J_{5/7,6}$ = 2.2 Hz, 2H, 5/7-H7, 4.30 (t, $J_{6,5/7}$ = 2.2 Hz, 1H, 6-H), 3.67 (s, 5H, Cp), 0.48 and 0.21 (s, and 6H each, α/δ-H and β/γ-H). – ^{29}Si NMR (THF, 30°C): δ = −18.4.

Reaction of a Mixture of **4a** *and* **4b** *with two Equivalents of n-Butyllithium:* At −78°C 1.8 ml of a 1.73 M solution of *n*BuLi in hexane was added to 0.85 g (1.6 mmol) of **4a** and **4b** dissolved in 50 ml of THF. When the temp. of the solution was raised slowly a yellow precipitate developed at −40°C and redissolved at room temp. After stirring for 1 h and cooling to −40°C overnight a solid was obtained from which the solvents were removed with a pipette. The remainder was washed three times with 20 ml of pentane and dried in vacuo to give 0.78 g of a yellow powder. When the powder was dissolved in [D_8]THF or a mixture of [D_8]THF and TMEDA the NMR signals expected for *bis(1,2,3,3a,8a-η⁵-3a,4,7a,8-tetrahydro-4,4,8,8-tetramethyl-4,8-disila-s-indacene-3a,7a-diyl)iron dianion* (**8**) and those of a trace of pentane were observed. – ^{1}H NMR ([D_8]THF/TMEDA, 25°C): δ = 6.30 (4H, 1/3-H), 6.11 (2H, 2-H), 4.04 (4H, 5/7-H), 3.52 (2H, 6-H), 0.53 and 0.10 (6H each, α/δ-H and β/γ-H).

Bis[(cyclopentadienyl)iron]-bis-μ-(1,2,3,3a,8a-η⁵-3a,4,7a,8-tetrahydro-4,4,8,8-tetramethyl-4,8-disila-s-indacene-3a,7a-diyl)chromium (**9**): To a solution of 1.7 g (7.0 mmol) of **1a** and **1b** in 150 ml of THF were added with stirring at −78°C 4.1 ml of a 1.70 M solution of *n*BuLi in hexane and, after warming to room temp., 30 ml of a 1.21 M solution of CpNa in THF and 6.0 g (13 mmol) of $Fe_2Cl_4(THF)_3$. The mixture was stirred for 1 h, the solvents were removed under reduced pressure, and the remainder was extracted with 300 ml of hexane. The resulting orange solution was cooled to −78°C, and 4.1 ml of a 1.70 M solution of *n*BuLi in hexane was added dropwise with stirring. When the mixture was warmed to room temp., a light orange cloudy precipitate formed. The liquid phase was removed with a cannula and the remainder washed with hexane until the solution was colorless. Addition of 200 ml of THF gave an orange solution that was separated from some solid material by cannula and treated with 0.7 g (3.5 mmol) of $CrCl_2(THF)$ to give a somewhat darker orange mixture. After stirring for 1 h the solvent was stripped in vacuo and the remainder extracted with 3 × 200 ml of hexane. Concentration of the combined extracts and slow cooling gave orange-red microcrystalline **9**. Yield 1.30 g (47% relative to **1a/b**); m.p. 155°C (dec.). – MS, *m/z* (%): 778 (100) [M^+], 389 (29) [M^{2+}], 364 (48) [CpFe(ligand)$^+$], 349 (23) [CpFe(ligand)$^+$ – CH_3]; isotope pattern of M^+, *m/z* (% calcd./found): 776 (16.6/18.1), 777 (12.4/13.6), 778 (100/100), 779 (76.6/77.7), 780 (44.4/44.1), 781 (18.2/18.4), 782 (6.0/7.8), 783 (1.3/2.8). – ^{1}H NMR ([D_8]toluene, 22°C): δ = 263 (5/7-H), 218 (6-H), 8.3 (2-H), 8.8 (Cp, 3.5 (1/3-H), 4.0 and -7.3 (CH_3); shifts relative to TMS, negative sign denotes low-frequency shifts.

$C_{38}H_{46}CrFe_2Si_4$ (778.5) Calcd. C 58.60 H 5.95 Cr 6.68
Found C 58.55 H 5.89 Cr 6.59

*Barrier to the Silatropic Rearrangement of syn-***3a/b**: For the signals of C-4a/7a and C-5/7 the coalescence temperature *T* was determined at different field strengths. The results are given in Table 5 together with the shift differences Δν taken from the low-temperature limiting spectra and the rate constants $k_c = 2^{-0.5} \cdot \pi \cdot \Delta\nu$; the error in *T* and Δν is 1.5 K and 1.5 Hz, respectively. When fitted to the Arrhenius equation these values gave E_a = 49.2 ± 2.9 kJmol^{-1}; 50.0 ± 9.2 kJmol^{-1} were obtained from the analysis of an Arrhenius plot.

Crystal Structure Determination: A suitable crystal of **3** was obtained by slow concentration of a solution in hexane. When three drops of TMEDA were added to a suspension of 0.15 g of the lithium derivative of **7** in 5 ml of Et_2O the salt dissolved partly. The mixture was heated under reflux, and small portions of Et_2O were added until a clear solution had formed. Slow cooling gave orange

Table 5. Coalescence parameters for *syn*-**3a/b** in C_6D_6

pair of nuclei	field [T]	temp. [K]	Δν [Hz]	k_c [1/s]
C-4a/7a	4.70	337.5	50.0	111.1
C-4a/7a	6.34	347.3	72.9	161.9
C-5/7	4.70	320.5	18.0	40.0
C-5/7	6.34	329.2	28.3	62.9

Table 6. Crystal structure data for *syn*-**3** and **7**Li(TMEDA)

	3	**7**Li(TMEDA)
formula	$C_{19}H_{24}FeSi_2$	$C_{25}H_{39}FeLiN_2Si_2$
M_r	364.422	486.561
crystal system	monoclinic	monoclinic
space group	$P2_1/c$(No.14)	$P2_1/c$(No.14)
a, Å	15.278(2)	12.910(2)
b, Å	8.934(2)	12.550(2)
c, Å	14.056(2)	17.586(2)
β, deg.	108.03(1)	106.40(1)
V, Å^3	1824.3	2733.4
Z	4	4
d_{calcd}, g/cm^3	1.327	1.182
μ(Mo-K_α), cm^{-1}	9.5	6,5
F(000), e	768	1040
T, °C	-50	-60
diffractometer	Syntex-$P2_1$	Enraf-Nonius CAD4
radiation	Mo-K_α, $\bar{\lambda}$ = 0.71069Å	
monochromator	graphite	
scan	ω	9/29
scan width (in ω)	0.8	0.8 + 0.35 tan ϑ
scan speed, °/min	0.7 - 29.3	1 - 10
$(\sin\vartheta/\lambda)_{max}$, Å^{-1}	0.595	0.595
hkl-range	+18, +10, ±16	±14, +12, +20
standard reflexions	2-50, 400, 006	2-50, 400, 006
refl. (measd./unique)	3550/3202	5088/4795
R_{int}	0.018	0.016
absorption correction	empirical	---
rel. transmission (min./max.)	0.74/1.00	---
refl. obs. [$F_o \geq 4.0\sigma(F_o)$]	2776	3856
structure solution	Patterson methods	
H atoms (found/calcd.)	16/8	16/7(16 neglected)
parameters ref.	199	250
$R^{a)}$	0.036	0.068
$wR^{b)}$	0.044	0.079
$\Delta\rho_{fin}$(max), e/Å^3	0.36/-0.29	1.38/-0.49

[a] $R = \Sigma(\|F_o\| - \|F_c\|)/\Sigma|F_o|$. – [b] $R_w = [\Sigma w(|F_o| - |F_c|)^2/\Sigma wF_o^2]^{1/2}$; $w = 1/\sigma^2(F_o)$.

Table 7. Fractional atomic coordinates and equivalent isotropic displacement parameters for *syn*-**3**

ATOM	X/A	Y/B	Z/C	U(eq.)
FE	0.15294(3)	0.13644(5)	0.15800(3)	0.018
SI1	0.20459(6)	0.51820(9)	0.14010(6)	0.027
SI2	0.36859(5)	0.27102(9)	0.29740(6)	0.023
C1	0.2485(4)	0.6327(4)	0.0539(3)	0.047
C2	0.0831(3)	0.5723(5)	0.1227(3)	0.062
C3	0.3988(3)	0.1082(4)	0.3858(3)	0.041
C4	0.4744(2)	0.3475(4)	0.2767(3)	0.035
C10	0.2806(2)	0.5446(3)	0.2705(2)	0.025
C11	0.3297(2)	0.6694(4)	0.3109(3)	0.030
C12	0.3856(2)	0.6420(4)	0.4124(3)	0.032
C13	0.3724(2)	0.4994(4)	0.4374(2)	0.032
C14	0.3087(2)	0.4239(4)	0.3492(2)	0.022
C20	0.2151(2)	0.3160(3)	0.1128(2)	0.020
C21	0.1614(2)	0.2296(3)	0.0288(2)	0.022
C22	0.1954(2)	0.0810(4)	0.0379(2)	0.021
C23	0.2702(2)	0.0720(4)	0.1279(2)	0.025
C24	0.2836(2)	0.2155(3)	0.1757(2)	0.022
C40	0.0775(2)	0.2129(4)	0.2464(2)	0.030
C41	0.0187(2)	0.1534(4)	0.1557(3)	0.032
C42	0.0427(2)	0.0011(4)	0.1487(2)	0.023
C43	0.1164(2)	-0.0342(4)	0.2368(2)	0.027
C44	0.1378(2)	0.0978(4)	0.2959(2)	0.027

Table 8. Fractional atomic coordinates and equivalent isotropic displacement parameters for **7Li**(TMEDA)

ATOM	X/A	Y/B	Z/C	U(eq.)
FE	0.20595(6)	0.19798(6)	0.09545(5)	0.041
SI1	0.2955(1)	0.3143(1)	0.28025(8)	0.046
SI2	0.3005(1)	0.4562(1)	0.10960(9)	0.044
C1	0.2252(6)	0.2178(5)	0.3294(4)	0.075
C2	0.4284(5)	0.3424(5)	0.3539(4)	0.086
C3	0.4354(5)	0.5247(5)	0.1448(5)	0.093
C4	0.2404(6)	0.4942(5)	0.0043(4)	0.080
C10	0.3238(4)	0.2520(4)	0.1917(3)	0.040
C11	0.3260(4)	0.3106(4)	0.1207(3)	0.040
C12	0.3438(5)	0.2328(5)	0.0658(3)	0.054
C13	0.3518(5)	0.1305(5)	0.1010(4)	0.071
C14	0.3404(5)	0.1422(4)	0.1782(4)	0.061
C20	0.0744(6)	0.1323(8)	0.1155(5)	0.089
C21	0.0610(5)	0.2394(9)	0.1075(7)	0.143
C22	0.0671(7)	0.2659(9)	0.032(1)	0.173
C23	0.0831(7)	0.171(1)	-0.0032(5)	0.089
C24	0.0863(7)	0.0917(7)	0.0496(8)	0.116
C30	0.2095(4)	0.4306(4)	0.2430(3)	0.042
C31	0.2090(4)	0.4863(4)	0.1702(3)	0.046
C32	0.1144(5)	0.5506(5)	0.1493(4)	0.077
C33	0.0583(5)	0.5367(5)	0.2062(4)	0.087
C34	0.1150(4)	0.4644(5)	0.2622(3)	0.059
N1	0.2869(4)	0.6612(4)	0.3878(3)	0.071
N2	0.2366(5)	0.7814(4)	0.2417(4)	0.102
LI	0.2173(8)	0.6138(7)	0.2673(6)	0.068
C1N1	0.399(1)	0.624(1)	0.4004(8)	0.065
C2N1	0.235(1)	0.606(1)	0.4470(9)	0.074
C3N1	0.276(1)	0.776(1)	0.3866(9)	0.080
C4N1	0.349(1)	0.770(1)	0.3897(8)	0.067
C5N1	0.206(1)	0.670(1)	0.4299(9)	0.079
C6N1	0.375(1)	0.587(1)	0.4353(8)	0.063
C1N2	0.1246(9)	0.8278(8)	0.2127(6)	0.128
C2N2	0.305(1)	0.793(1)	0.1874(8)	0.167
C3N2	0.2889(7)	0.8318(7)	0.3194(5)	0.093

crystals of **7Li**(TMEDA). Table 6 contains compilation of data relevant to the crystal structure determinations. In Tables 7 and 8 are listed the atomic coordinates of the non-H atoms. Further crystal structure data have been deposited[24].

CAS Registry Numbers

1a: 75794-33-1 / **1b**: 75794-34-2 / **2Li**: 133191-61-4 / *syn*-**3a**: 133191-62-5 / **4** (isomer 1): 133191-63-6 / **4** (isomer 2): 133191-64-7 / **5**: 133191-69-2 / **7Li**: 133191-65-8 / **7Li** (TMEDA): 133191-68-1 / **8Li$_2$**: 133191-66-9 / **9**: 133191-67-0 / CpNa: 4984-82-1 / $Fe_2Cl_4(THF)_3$: 12562-70-8 / ^{29}Si: 14304-87-1

[1] [1a] C. E. Carraher, Jr., J. E. Sheats, C. U. Pittman, Jr. (Eds.), *Organometallic Polymers*, Academic Press, New York 1978. — [1b] R. B. Seymour (Ed.), *Conductive Polymers*, Plenum Press, New York 1981. — [1c] C. E. Carraher, Jr., J. E. Sheats, C. U. Pittmann, Jr. (Eds.), *Advances in Organometallic and Inorganic Polymer Science*, Marcel Dekker Inc., New York 1982. — [1d] J. E. Sheats, C. E. Carraher, Jr., C. U. Pittmann, Jr (Eds.), *Metal-Containing Polymer Systems*, Plenum Press, New York 1985.

[2] C. E. Carraher, Jr., R. J. Linville, T. A. Manek, H. S. Blaxall, J. R. Taylor, L. P. Torre in ref.[1b], p. 77; T. E. Bitterwolf in ref.[1d], p. 137; H. Yasuda, I. Noda, Y. Morita, H. Nakamura, S. Miyanaga, A. Nakamura, *ibid.*, p. 275.

[3] R. Liepins, M. L. Timmons, M. Morosoff, J. Surless, in ref.[1d], p. 225.

[4] R. H. Grubbs, S.-C. H. Su in ref.[1a], p. 129; W. H. Lang, A. T. Jurewicz, W. O. Haag, D. D. Whitehurst, L.D. Rollmann, *ibid.*, p. 145; C. Carlini, G. Sbrana in ref.[1c], p. 323; D. W. Slocum, B. Conway, M. Hodgman, K. Kuchel, M. Moronski, R. Noble, K. Webber, S. Duraj, A. Siegel, D. A. Owen, *ibid.*, p. 357.

[5] G. M. Brown, R. W. Callahan, E. C. Johnson, T. J. Meyer, T. R. Weaver in *Extended Interactions between Metal Ions* (L. V. Interrante, Ed.), p. 66, American Chemical Society, Washington, D.C., 1974.

[6] G. Sekutowski, R. Jungst, G. D. Stucky in ref.[5], p. 142.

[7] Y. Nakadaira, H. Sakaba, H. Sakurai, *Chem. Lett.* **1980**, 1071; T. J. Barton, G. T. Burns, E. V. Arnold, J. Clardy, *Tetrahedron Lett.* **22** (1981) 7; N. N. Zemlyanskii, I. V. Borisova, Yu. N. Luzikov, Yu. A. Ustynyuk, N. D. Kolosova, I. P. Beletskaya, *J. Org. Chem. USSR, Engl. Transl.*, **17** (1981) 1174; P. R. Jones, J. M. Rozell, Jr., B. M. Campbell, *Organometallics* **4** (1985) 1321.

[8] J. Hiermeier, F. H. Köhler, G. Müller, *Organometallics*, in press.

[9] H. Atzkern, J. Hiermeier, F. H. Köhler, A. Steck, *J. Organomet. Chem.*, in press; J. Hiermeier, *Dissertation*, Techn. Univ. München, 1989.

[10] P. Jutzi, *Chem. Rev.* **86** (1986) 983.

[11] D. Marquarding, H. Klusacek, G. Gokel, P. Hoffmann, I. Ugi, *J. Am. Chem. Soc.* **92** (1970) 5389.

[12] [12a] F. A. L. Anet, V. J. Basus, *J. Magn. Reson.* **32** (1978) 339. — [12b] N. Okzawa, T. S. Sorensen, *Can. J. Chem.* **56** (1978) 2737.

[13] Yu. K. Grishin, Yu. N. Luzikov, Yu. A. Ustynyuk, *Dokl. Chem., Engl. Transl.* **216** (1974) 315.

[14] [14a] T. D. Turbitt, W. E. Watts, *Tetrahedron* **28** (1972) 1227. — [14b] B. Fuchs, R. Fröhlich, H. Musso, *Chem. Ber.* **118** (1985) 1968.

[15] C. Elschenbroich, J. Schneider, H. Prinzbach, W.-D. Fessner, *Organometallics* **5** (1986) 2091.

[16] D. De Montanzon, R. Poilblanc, P. Lemoine, M. Gross, *Electrochim. Acta* **23** (1978) 1247.

[17] V. K. Belsky, N. N. Zymlianski, I. V. Borisova, N. D. Kolosova, I. P. Beletskaya, *Cryst. Struct. Commun.* **11** (1982) 497.

[18] P. Seiler, J. D. Dunitz, *Acta Crystallogr., Sect. B*, **35** (1979) 2020.

[19] M. F. Lappert, A. Singh, L. M. Engelhardt, A. H. White, *J. Organomet. Chem.* **262** (1984) 271; P. Jutzi, E. Schlüter, S. Pohl, W. Saak, *Chem. Ber.* **118** (1985) 1959.

[20] P. Seiler, J. D. Dunitz, *Acta Crystallogr., Sect. B*, **35** (1979) 1068; F. Takusagawa, T. F. Koetzle, *ibid.* **35** (1979) 1074.

[21] F. H. Köhler, *J. Organomet. Chem.* **110** (1976) 235; F. H. Köhler, W. A. Geike, *ibid.* **238** (1987) 35.

[22] F. H. Köhler, K. H. Doll, W. Prößdorf, *J. Organomet. Chem.* **224** (1982) 341.

[23] N. Hebendanz, F. H. Köhler, F. Scherbaum, B. Schlesinger, *Magn. Reson. Chem.* **27** (1989) 789.

[24] Fachinformationszentrum Karlsruhe, Gesellschaft für wissenschaftlich-technische Information mbH, D-7514 Eggenstein-Leopoldshafen 2 (FRG). Inquiries should be accompanied by the depository number CSD-55318, the names of the authors and the literature citation.

[34/91]